Published in final edited form as:
Chem Res Toxicol. 2010 January 18; 23(1): 11–19. doi:10.1021/tx9004264.

Efficient Formation of the Tandem Thymine Glycol/8-oxo-7,8-dihydroguanine Lesion in Isolated DNA and the Mutagenic and Cytotoxic Properties of the Tandem Lesions in *Escherichia coli* Cells

Bifeng Yuan[1,§], **Yong Jiang**[2,§], **Yuesong Wang**[1], and **Yinsheng Wang**[1,2,*]

[1] Department of Chemistry, University of California, Riverside, CA 92521-0403

[2] Environmental Toxicology Graduate Program, University of California, Riverside, CA 92521-0403

Abstract

Reactive oxygen species can induce the formation of not only single-nucleobase lesions, which have been extensively studied, but also tandem lesions. Herein we report a high frequency of formation of a type of tandem lesion, where two commonly observed oxidatively induced single-nucleobase lesions, i.e., thymidine glycol (Tg) and 8-oxo-7,8-dihydro-2′-deoxyguanosine (8-oxodG) are vicinal to each other, in calf thymus DNA upon exposure to Cu(II)/ascorbate along with H_2O_2 or γ rays. We further explored how the tandem lesions perturb the efficiency and fidelity of DNA replication by assessing the replication products formed from the propagation, in *Escherichia coli* cells, of the single-stranded pYMV1 shuttle vectors containing two tandem lesions [5′-(8-oxodG)-Tg-3′ and 5′-Tg-(8-oxodG)-3′] or an isolated Tg or 8-oxodG. The bypass efficiencies for the two tandem lesions were approximately one half of those for the two isolated single-nucleobase lesions. The presence of an adjacent Tg could lead to significant increases in G→T transversion at the 8-oxodG site compared to that of a single 8-oxodG lesion; the frequencies of G→T mutation were approximately 18%, 32% and 28% for 8-oxodG that are isolated, in 5′-(8-oxodG)-Tg-3′ and in 5′-Tg-(8-oxodG)-3′, respectively. Moreover, both pol IV and pol V are involved, in part, in bypassing the Tg, either present alone or as part of the tandem lesions, in *Escherichia coli* cells. Together, our results support that complex lesions could exert greater cytotoxic and mutagenic effects than when the composing individual lesions are present alone.

Introduction

The integrity of the human genome is constantly challenged by endogenous and exogenous agents, among which reactive oxygen species (ROS)[1] can be produced from normal aerobic metabolism or from exposure to ionizing radiation and antitumoral agents (1). In this regard, ROS include hydroxyl radical, superoxide radical, hydrogen peroxide, and singlet oxygen; they can react directly with DNA (i.e., hydroxyl radical and singlet oxygen) or modify DNA when

*Address correspondence to: Yinsheng Wang, Department of Chemistry-027, University of California, Riverside, CA 92521-0403. Telephone: (951)827-2700. Fax: (951)827-4713. yinsheng.wang@ucr.edu.

§B.Y. and Y.J. contributed equally to this work

Supporting Information Available: LC-MS/MS results and calibration curves. This material is available free of charge via the Internet at http://pubs.acs.org.

[1]**Abbreviations:** ROS, Reactive oxygen species; Tg, 5,6-dihydroxy-5,6-dihydrothymidine; 8-oxodG, 8-oxo-7,8-dihydro-2′-deoxyguanosine; ODN, oligodeoxyribonucleotide; CRAB, competitive replication and adduct bypass; REAP, restriction endonuclease and post-labeling.

in the presence of transition metal ions (i.e., hydrogen peroxide and superoxide radical) (1,2). The accumulation of ROS-induced DNA lesions may bear important implications in the pathogenesis of a number of human diseases including cancer and neurodegeneration (2).

Other than single-nucleobase lesions, clustered DNA lesions, where two or more damaged nucleosides are located within 1–2 helical turns of DNA, can form upon interaction with ROS, particularly those formed upon exposure to ionizing radiation (3–5). Copper is known to be associated with chromatin (6) and it can form stable complexes with DNA (7–10). Studies showed that copper plays a significant role in H_2O_2-mediated DNA damage (11–14). *In vitro* studies showed that Cu(II) and H_2O_2, frequently together with the presence of ascorbate, induce DNA strand breaks as well as many types of single-nucleobase and intrastrand crosslink lesions (12,13,15–18).

Due to the intrinsic chemical and structural properties of different lesions and their close proximity, clustered DNA lesions often display altered mutagenic potential (19,20) and are more difficult to repair than when they are present alone (21–26). As a subset of clustered lesions, tandem lesions, comprising of two contiguously damaged nucleotides, can emanate from ROS attack (12,13,27–36). One type of tandem lesion, with an 8-oxo-7,8-dihydro-2′-deoxyguanosine (8-oxodG) and a formamido (dβF) moiety being adjacent to each other, was first found to form in short oligodeoxyribonucleotides (ODNs) upon exposure to γ rays or Fenton-type reagents under aerobic conditions (37,38). Later it was observed that the amounts of these tandem lesions, with dβF being adjacent to 8-oxodG, formed in isolated DNA upon γ ray exposure cannot account for the total amount of tandem lesions involving 8-oxodG (32). It was, thus, concluded that other tandem lesions involving 8-oxodG may exist (32). Since 5,6-dihydroxy-5,6-dihydrothymidine (or thymidine glycol, Tg) and 8-oxodG are major single-nucleobase lesions induced by ROS from thymidine and 2′-deoxyguanosine, respectively (23,39,40), we reason that tandem lesions with an 8-oxodG being adjacent to a Tg might be induced in DNA by ROS.

Tg can block effectively DNA replication *in vitro* (41,42) and it exhibits a low mutagenic potential (39). The 8-oxodG, on the other hand, does not block DNA replication, but is mutagenic in many systems, which can result in both G→T and G→C mutations, with the former being more prevalent (43,44). Thymidine glycol could also arise from the deamination of 5-methylcytosine glycol, a common oxidatively induced lesion of 5-methylcytosine (Figure 1) (18,45). Thus, the 5′-Tg-(8-oxodG)-3′ tandem lesion may form from ROS attack at methylated CpG site and contribute to CpG mutagenesis (18,46).

We recently showed that the tandem lesions composed of Tg and 8-oxodG exhibit stronger blocking effects toward DNA replication mediated by purified DNA polymerases *in vitro* than when either lesion is present on its own (47). In addition, steady-state kinetic studies revealed that the mutagenic properties of isolated Tg or 8-oxodG are different from when they are adjacent to each other (47). However, it is not clear whether the above findings can be extended to cells.

In the present paper, we assessed quantitatively the formation of the tandem 5′-Tg-(8-oxodG)-3′ lesion in isolated DNA. We also prepared single-stranded pYMV1 shuttle vectors containing a 5′-(8-oxodG)-Tg-3′, 5′-Tg-(8-oxodG)-3′, or an isolated Tg or 8-oxodG at a defined site and assessed how these lesions compromise the efficiency and fidelity of DNA replication in *E. coli* cells.

Materials and Methods

Materials

Copper (II) chloride, L-methionine, L-ascorbic acid and calf thymus DNA were from Sigma-Aldrich (St. Louis, MO). Hydrogen peroxide (30%) and nuclease P1 were purchased from Fisher Scientific (Fair Lawn, NJ) and MP Biomedicals (Aurora, OH), respectively. Unmodified ODNs used in this study were purchased from Integrated DNA Technologies (Coralville, IA), and [γ-^{32}P]ATP was obtained from Perkin Elmer (Piscataway, NJ). 1,1,1,3,3,3-hexafluoro-2-propanol (HFIP) was purchased from TCI America (Portland, OR). Shrimp alkaline phosphatase was obtained from USB Corporation (Cleveland, OH); all other enzymes were from New England Biolabs (Ipswich, MA). The single-stranded pYMV1 vector and the wild-type AB1157 *E. coli* strain were kindly provided by Prof. Peter E.M. Gibbs (48) and Prof. John M. Essigmann, respectively. The polymerase-deficient AB1157 strains [Δ*pol B1*::spec (pol II-deficient), *ΔdinB* (pol IV-deficient), *ΔumuC*::kan (pol V-deficient) and *ΔumuC*::kan *ΔdinB* (pol IV, pol V-double knockout)] were generously provided by Prof. Graham C. Walker (49).

Treatment of calf thymus DNA

Calf thymus DNA was desalted by ethanol precipitation. The DNA pellet was redissolved in a solution containing 100 mM NaCl, 1 mM EDTA and 10 mM Tris-HCl (pH 7.5), and the DNA was annealed by heating the solution to 90 °C and cooling slowly to room temperature. Aliquots of DNA (150 μg) were incubated with $CuCl_2$ (12.5–200 μM), H_2O_2 (0.1–1.6 mM), and ascorbate (1–16 mM) in a 0.5-mL solution at room temperature for 50 min (The concentrations of individual Fenton reagents are shown in Table 1). In this respect, chemicals used in Fenton-type reaction were freshly dissolved in doubly distilled water and the reactions were carried out under aerobic conditions. The reactions were terminated by adding an excess amount of L-methionine, and the resulting DNA samples were desalted by ethanol precipitation and quantified by measuring the UV absorbance at 260 nm.

For the treatment with γ rays, calf thymus DNA (50 μg) was first dissolved in a 250-μL solution containing 50 mM NaCl and 10 mM phosphate (pH 7.0), Cu(II), and ascorbate at concentrations shown in Table 1. The resulting solution was exposed to γ rays delivered by a Mark I ^{137}Cs irradiator (JL Shepherd and Associates, San Fernando, CA). The samples were treated with γ rays at a total dose of 50 Gy over a period of 20 min. The γ ray-exposure experiments were also carried out in the presence of 50 μM Cu(II), 4 mM ascorbate, or both. After the γ ray exposure, the DNA samples were desalted by ethanol precipitation and quantified.

Enzymatic digestion of calf thymus DNA

To the above treated DNA (20 μg) were added 2 units of nuclease P1 and a 30-μL buffer solution containing 300 mM sodium acetate (pH 5.0) and 10 mM zinc acetate. The digestion was continued at 37 °C for 4 hrs, and the enzyme in the resulting digestion mixtures was removed by chloroform extraction. The amount of nucleosides in the mixture was quantified by UV absorbance measurements, and aliquots of the nucleoside mixture were subjected directly to LC-MS/MS analysis.

Quantitative LC-MS/MS analysis

LC-MS/MS quantification was performed by using an Agilent 1100 capillary HPLC pump (Agilent Technologies, Santa Clara, CA) interfaced with an LTQ linear ion-trap mass spectrometer (Thermo Fisher Scientific, San Jose, CA). A 0.5×250 mm Zorbax SB-C18 column (5 μm in particle size, Agilent Technologies) was used for the separation of the DNA hydrolysates, and the flow rate was 7.0 μL/min. A 10-min gradient of 0–20% methanol in 400 mM HFIP (pH was adjusted to 7.0 by addition of triethylamine), followed by a 30-min gradient

of 20–50% methanol in 400 mM HFIP, was used for the separation. The mass spectrometer was set up for monitoring the fragmentation of the $[M - H]^-$ ions of 2′-deoxyadenosine-5′-phosphate (pdA) and dinucleotides pTg-p(8-oxodG) and pTg-pdG. The capillary temperature for the electrospray source of the mass spectrometer was maintained at 300 °C to minimize the formation of the HFIP adducts of nucleotides.

Construction of calibration curves for the quantifications of the 5′-Tg-(8-oxodG)-3′ tandem lesion and isolated Tg lesion

Certain amounts of tandem lesion-containing dodecameric standard, d(ATGGCTgG*GCTAT) [‘G*’ represents an 8-oxodG, and ‘Tg’ represents the *cis*-(*5R,6S*) diastereomer of Tg], or single Tg lesion-bearing dodecameric standard, d(ATGGCTgGGCTAT) (50), were mixed with 20 μg of untreated calf thymus DNA. The resulting DNA was enzymatically digested following the same methods as described above and the samples were subjected to LC-MS/MS analysis.

Preparation of lesion-bearing ODN substrates

The above described 12mer lesion-bearing substrates were ligated with the 5′-phosphorylated d(GTATCCTCC) in the presence of a template ODN, d (TTTTATAGCACGCCATGGAGGATACTTTT), following previously described procedures (33). The resulting lesion-containing 21-mer ODNs (sequences shown in Table S1) were purified by using 20% denaturing polyacrylamide gel electrophoresis (PAGE) and desalted by ethanol precipitation. The integrity and purity of the ligation products were further confirmed by LC-MS/MS and PAGE analysis.

Construction of ss-pYMV1 genomes harboring a site-specifically inserted 8-oxodG, Tg, 5′-(8-oxodG)-Tg-3′, or 5′-Tg-(8-oxodG)-3′

The lesion-containing single-stranded pYMV1 viral genomes and the control lesion-free genome were prepared following the previously described procedures (51). Briefly, 20 pmol of pYMV1 vector was digested with 40 U EcoRI at 23°C for 8 hrs to linearize the vector. Two scaffolds, 5′-ATGGAGGATACCACTGAATCATGGTCATAGC-3′ and 5′-AAAACGACGGCCAGTGAATTATAGC-3′ (25 pmol), each spanning one end of the linearized vector and the modified ODN insert, were annealed with the linearized pYMV1 vector. The 21mer control or lesion-containing inserts were 5′-phosphorylated with T4 polynucleotide kinase and subsequently ligated to the above vector by using T4 DNA ligase at 16°C for 8 hrs. T4 DNA polymerase (22.5 U) was subsequently added and the solution was incubated at 37°C for 4 hrs to digest the scaffolds and residual unligated pYMV1 vector. The constructed genomes were normalized against a lesion-free competitor genome (51,52), which was prepared by inserting a 24mer unmodified ODN, 5′-GTATCCTCCATGGCACAGCGCTAT-3′, to the EcoRI-linearized genome.

Transfection of E. coli cells with ss-pYMV1 vectors containing an 8-oxodG, Tg, 5′-(8-oxodG)-Tg-3′ or 5′-Tg-(8-oxodG)-3′

Purified control or lesion-containing genome (150 fmol) was mixed with the competitor genome at a molar ratio of 6:1 (lesion/competitor) and transfected into the AB1157 *E. coli* cells by electroporation. The *E. coli* cells were then grown in 3-mL LB medium at 37°C for 6 hrs and the phage was recovered from the supernatant by centrifugation at 13,000 rpm for 5 min. The resulting phage was further amplified in SCS110 *E. coli* cells to increase the progeny/lesion-genome ratio (51,52). After the phage was recovered from the supernatant, the progenies of the pYMV1 vector were isolated using QIAprep Spin M13 kit (Qiagen, Valencia, CA).

Determination of the bypass efficiency and mutation frequency using competitive replication and adduct bypass (CRAB) and restriction endonuclease and post-labeling (REAP) assays

CRAB and REAP assays were carried out to examine the bypass efficiency and mutation frequency according to the previously described procedures (51–53) with some modifications (34,54,55). PCR amplification of the region of interest in the resulting isolated progeny genome was performed by using Phusion high-fidelity DNA polymerase. The primers were 5′-YCAGCTATGACCATGATTCAGTGGTATCCTCC-3′ and 5′-Y TCGGTGCGGGCCTCTTCGCTATTAC-3′ (‘Y’ is an amino group), and the amplification conditions consisted of 10 s at 98 °C, 30 s at 62 °C, 15 s at 72 °C for 30 cycles, followed by a final extension at 72 °C for 5 min. The PCR products were purified by using QIAquick PCR purification kit (Qiagen, Valencia, CA).

For the bypass efficiency assay, 5% of the above PCR products was treated with 10 U NcoI and 1 U shrimp alkaline phosphatase in a 10-μL NEB buffer 2 at 37°C for 2 hrs, followed by heating at 65 °C for 20 min to deactivate the phosphatase. The mixture was then treated in a 15-μL NEB buffer 2 containing 5 mM DTT, ATP (50 pmol cold, premixed with 1.66 pmol [γ-^{32}P] ATP) and 10 U polynucleotide kinase. The reaction was continued at 37°C for 1 hr, followed by heating at 65 °C for 20 min to deactivate the polynucleotide kinase. To the above reaction mixture was added Tsp509I (10 U) and the solution was incubated at 65 °C for 1 hr, followed by quenching with 15 μL formamide gel loading buffer containing xylene cyanol FF and bromophenol blue dyes. The mixture was resolved by using 30% native polyacrylamide gels (acrylamide:bis-acrylamide=19:1) and quantified by phosphorimager analysis. After the restriction enzyme cleavages, the DNA fragment of interest from the full-length replication product was liberated as an 13mer ODN, d(p*CATGGC**MN**GCTAT), where “MN” designates the nucleobases present at the original 5′-(8-oxodG)-dT-3′, 5′-Tg-dG-3′, 5′-(8-oxodG)-Tg-3′ or 5′-Tg-(8-oxodG)-3′ site after *in vivo* DNA replication and ‘p*’ represents the 5′-radiolabeled phosphate. The 13mer with a single-nucleotide difference could be resolved by 30% native polyacrylamide gels. On the other hand, the corresponding DNA fragment released from the competitor genome was a 16mer ODN, d(p*CATGGCACAGCGCTAT). The mutation frequencies were determined from the relative amounts of different 13mer products from the gel band intensities. The bypass efficiency was calculated using the following formula, % bypass= (lesion signal/competitor signal)/(non-lesion control signal/its competitor signal) (51).

Identification of replication products by using LC-MS/MS

In order to identify the replication products using LC-MS/MS, 80% of the above PCR products were treated with 50 U NcoI and 20 U shrimp alkaline phosphatase in 200-μL NEB buffer 2 at 37°C for 2 hrs, followed by heating at 65°C for 20 min. To the resulting solution was added Tsp509I (50 U), and the reaction mixture was incubated at 65°C for 1 hr followed by extraction with phenol/chloroform/isoamyl alcohol (25:24:1, v/v), and the aqueous portion was dried with Speed-vac and dissolved in water. The resulting mixture was subjected to LC-MS/MS analysis. A 0.5×150 mm Zorbax SB-C18 column (Agilent Technologies) was used for the separation, the flow rate was 8.0 μL/min, and a 5-min gradient of 0–20% methanol followed by a 35-min of 20–50% methanol in 400 mM HFIP was employed for the separation. The LTQ linear ion trap mass spectrometer was set up for monitoring the fragmentation of the [M-3H]$^{3-}$ ions of the 13mer [d(CATGGC**MN**GCTAT), where ‘**MN**’ designates GT, TT, CT, or TG and 16mer [i.e., d(CATGGCACAGCGCTAT)] ODNs.

Results

Quantitative measurement of the formation of tandem single-nucleobase lesions in DNA by LC-MS/MS necessitates the development of enzymatic digestion procedures for the selective

release of the tandem lesion as a unique chemical entity. To this end, we took advantage of the previous observation that thymidine glycol prohibits the cleavage of its 3′ phosphodiester linkage by nuclease P1 (56), and employed this enzyme to liberate the tandem 5′-Tg-(8-oxodG)-3′ lesion from DNA as a dinucleotide. Under this digestion condition, an isolated Tg is also released along with its 3′ flanking undamaged nucleoside as a dinucleotide.

We supplemented calf thymus DNA with different amounts of an authentic dodecameric ODN carrying an isolated thymidine glycol (5′-Tg-dG-3′) or the 5′-Tg-(8-oxodG)-3′ tandem lesion. We then digested the DNA mixture with nuclease P1, removed the enzyme, and subjected it to LC-MS/MS analysis, where we monitored specifically the fragmentation of the $[M - H]^-$ ions of 2′-deoxyadenosine-5′-phosphate (pdA) and Tg-carrying dinucleotide, namely, 5′-pTg-p(8-oxodG)-3′ (Figure S1), for the tandem lesion-carrying substrate, or 5′-pTg-pdG-3′, for the substrate containing a Tg situating on the 5′ side of an unmodified dG. The ratio for the peak areas found in the extracted-ion chromatogram for monitoring the fragmentation of the dinucleotide over that for pdA was then plotted against the amount of Tg- or 5′-Tg-8-oxodG-3′-bearing substrate that we added, which afforded straight lines for both types of lesion-containing substrates (Figure S2). These results support that nuclease P1 digestion combined with LC-MS/MS analysis can allow for a reliable quantification of the thymidine glycol lesion, which is present on the 5′ side of an unmodified nucleoside or 8-oxodG. In this respect, we normalized the ion currents of the analytes to that of pdA to correct for the variation in sample loading and analyte loss during the sample preparation.

After having established an analytical method for monitoring the formation of the tandem 5′-Tg-(8-oxodG)-3′ lesion and Tg followed by an unmodified dG, we demonstrated the formation of these two types of lesions in calf thymus DNA treated with Cu(II)/H_2O_2/ascorbate (Figure S1). In addition, quantification results revealed the dose-responsive formation of both lesions (Figure 2A). To our surprise, we observed that the yield of the tandem lesion, 5′-Tg-(8-oxodG)-3′, was merely 5–6 fold lower than what was found for the Tg that is situated on the 5′ side of an unmodified dG (Figure 2A).

Our experimental results also showed that copper ions, especially Cu(I), could stimulate the γ ray-induced formation of the 5′-Tg-(8-oxodG)-3′ tandem lesion (Figure 2B&C). In this regard, we exposed calf thymus DNA to 50 Gy of γ rays in the presence of increasing concentrations of Cu(II) and ascorbate, and quantified the Tg and Tg-(8-oxodG) lesions by LC-MS/MS. The presence of Cu(II) and ascorbate enhanced markedly the γ ray-mediated formation of both types of lesions. For instance, the amount of the 5′-Tg-(8-oxodG)-3′ formed in the presence of 200 μM of Cu(II) and 16 mM of ascorbate is approximately 400 times higher than that induced by γ rays alone (Figure 2B). To gain further insights into the Cu(II)/ascorbate-enhanced formation of these lesions, we also compared the yields for the formation of lesions in calf thymus DNA upon treatment with 50 Gy of γ rays in the presence of 50 μM Cu(II), 4 mM ascorbate, or both. It turned out that, while the presence of ascorbate inhibited considerably the formation of both types of lesions, the existence of Cu(II) stimulated significantly the formation of these lesions. The presence of both Cu(II) and ascorbate, which reduces Cu(II) to Cu(I), further enhanced the formation of both types of lesions (Figure 2C). These results support without ambiguity the role of Cu(I) in enhancing the γ ray-mediated formation of these lesions.

We next investigated the mutagenic and cytotoxic properties of the tandem lesions, where the Tg and 8-oxodG are adjacent to each other, as well as the isolated Tg and 8-oxodG in *E. coli* cells. To this end, we prepared the lesion-carrying 21-mer substrates by enzymatic ligation (Table S1), confirmed the identities of the 21-mer ODNs by ESI-MS and MS/MS (Figures S3-S6), and inserted the above 21mer lesion-containing ODNs into the single-stranded pYMV1 genome. We next assessed the bypass efficiencies and mutation frequencies of these DNA

lesions by using the CRAB and REAP assays introduced by Essigmann and coworkers (Figure 3) (51–53) with some modifications (34,55). A unique feature of these assays lies in that the entire progeny population was used for determining the mutation frequency and bypass efficiency, thereby offering statistically sound conclusions (51); additionally, the methods do not require phenotypic selection (51).

Restriction digestion of the PCR products of the progeny pYMV1 genome resulting from *in-vivo* replication renders 13mer fragment(s) harboring the site where the single or tandem lesions were initially incorporated. The corresponding digestion of PCR products of the progeny of the competitor genome gives a 16mer fragment (Figure 3). The failure to detect radio-labeled fragments with lengths shorter than 13mer supports that none of the single or tandem lesions give rise to deletion mutations (Figure 4 and Figure S9). In this context, we employed 30% (19:1, acrylamide:bisacrylamide) non-denaturing polyacrylamide gels to resolve the ^{32}P-labeled fragments; the 13mers with a single nucleotide difference can be resolved from each other (Figure 4).

It is worth noting that the identities of the above restriction fragments were confirmed by LC-MS/MS analyses (34). In this context, we were able to detect the 13mer ODNs d (CATGGC**MN**GCTAT) [‘**MN**’ is GT or TT for the isolated 8-oxodG-bearing substrate; GT for the isolated Tg-bearing substrate; GT or TT for 5′-(8-oxodG)-Tg-3′; and TG or TT for 5′-Tg-(8-oxodG)-3′] in the restriction digestion mixtures (Some example LC-MS and MS/MS results are depicted in Figure S7), which is consistent with the findings made from native PAGE analysis.

The bypass efficiencies were calculated from the ratio of the combined intensities of bands observed for the 13mer products, which were from the replication of the lesion genome, over the intensity of the 16mer band, from the replication of the competitor genome, with the consideration of the ratio of the lesion over competitor genomes employed during the initial transfection. The bypass efficiencies for the lesion-carrying genomes were then normalized against that for the control lesion-free genome.

The results showed that the bypass efficiencies for the tandem lesions are about one half of those for the isolated Tg or 8-oxodG in all AB1157 strains that we examined (Figure 5A). The bypass efficiencies for the isolated 8-oxodG, isolated Tg, 5′-(8-oxodG)-Tg-3′ and 5′-Tg-(8-oxodG)-3′ in wild-type AB1157 cells were ~109%, 96%, 46% and 38%, respectively (Figure 5A). Deficiency in pol II in the isogenic AB1157 background does not affect appreciably the bypass efficiencies of Tg or 8-oxodG, either present alone or in tandem (Figure 5A and Table S2). However, the bypass efficiencies for Tg, 5′-(8-oxodG)-Tg-3′ and 5′-Tg-(8-oxodG)-3′ dropped in the isogenic AB1157 cells deficient in pol IV, pol V, or both. These data support that both pol IV and pol V are involved partially in the bypass of Tg, 5′-(8-oxodG)-Tg-3′ and 5′-Tg-(8-oxodG)-3′ in *E. coli* cells.

The results from native PAGE analysis also allowed us to measure the mutation frequencies of these lesions in wild-type and DNA polymerase-deficient AB1157 *E. coli* strains (49). The quantification data showed that the 8-oxodG, when isolated or present in the 5′-(8-oxodG)-Tg-3′ or 5′-Tg-(8-oxodG)-3′, are mutagenic in wild-type AB1157 cells, with G→T transversion occurring at frequencies of 18%, 32% and 28%, respectively. Thus, the presence of an adjacent Tg can lead to a significant increase in G→T transversion at the 8-oxodG site. However, deficiency in SOS-induced polymerases does not result in considerable change in G→T mutation induced by 8-oxodG, regardless it is isolated or adjacent to a Tg in the 5′-(8-oxodG)-Tg-3′ or 5′-Tg-(8-oxodG)-3′ (Figure 5B). At first glance, the observation of decreased bypass efficiencies of the two tandem lesions in pol IV- or pol V-deficient background appears to be inconsistent with the lack of increase in mutation frequencies of the two tandem lesions when

replicated in pol IV- or pol V-deficient cells. We, however, reason that pol IV and pol V may play an important role in bypassing the Tg component of the tandem lesions, whereas the bypass of the 8-oxodG portion may not require significant participation of pol IV or pol V. This may explain the lack of influence of these two polymerases on the mutation frequencies observed for the 8-oxodG component of the two tandem lesions. In support of this argument, we indeed observed a compromised bypass of isolated Tg in pol IV- or pol V-defective background; however, the bypass efficiency of 8-oxodG is not substantially altered by the deficiency of either polymerase (Figure 5A and Table S2). It is worth emphasizing that the above replication experiments were carried out in *E. coli* strains without SOS induction; SOS induction is known to stimulate substantially the expression of pol IV and pol V (49). Thus, we would expect to observe more pronounced difference in bypass efficiency, and possibly mutation frequency, between wild-type and pol IV- or pol V-deficient *E. coli* cells upon SOS induction, as observed with other Tg-containing tandem lesions (57). Further experiments are needed to reveal whether this is the case.

Discussion

Copper is known to associate with chromatin (6), and the binding constants of Cu(I) and Cu (II) with DNA are 10^9 and 10^4 M (7,15), respectively. In the reducing cytosolic environment of prokaryotic and eukaryotic cells, most copper ions, mainly in the form of Cu(I), are complexed with cysteine or methionine residues in copper transporting or binding proteins; there are few if any copper ions that are thought to be ‘free’ in terms of thermodynamic availability and reaction chemistry (58). The changing cellular environments (e.g. oxidative bursts), however, may result in the oxidation of the ligating groups, thereby disrupting the binding sites, liberating the Cu(I) ions, and inducing the vicious cycles of toxic ROS formation (58). Therefore, it is important to investigate how the presence of copper ions affects oxidative DNA damage.

The availability of ODNs containing both Tg and 8-oxodG (50) facilitated us to develop an LC-MS/MS method to quantify the formation of the tandem lesion where a Tg lies on the 5′ side of an 8-oxodG and allowed us to assess the mutagenicity and cytotoxicity of the tandem lesions composed of Tg and 8-oxodG. We found that the tandem lesion, where a Tg lies on the 5′ side of an 8-oxodG, could be induced, at a relatively high yield (i.e., about 5–6 fold less than an isolated Tg situated on the 5′ side of an unmodified dG), in calf thymus DNA upon exposure to Cu(II)/ascorbate along with H_2O_2 or γ rays. The exact mechanism for the efficient formation of the 5′-Tg-(8-oxodG)-3′ remains unclear, and further studies are needed.

Thymidine glycol and 8-oxodG are two major DNA lesions induced by ROS. *In-vitro* primer extension assay with exonuclease-free Klenow fragment and yeast polymerase η showed that the presence of the tandem lesion containing both Tg and 8-oxodG in template DNA blocks the progression of DNA replication more readily than when the two lesions were present alone (47). The mutagenic properties of the tandem lesions, as revealed by steady-state kinetic assay, also differ from the two composing lesions when exist on their own (47). Moreover, it was found that the cleavage of 8-oxodG by hOGG1 was inhibited substantially by the presence of a neighboring 5′ Tg (47), indicating that the tandem lesion might be more resistant to repair.

To explore whether the above findings about the replication of the tandem lesions can be extended to cells, here we investigated the mutagenic and cytotoxic properties of the tandem lesions in *E. coli* cells by using single-stranded pYMV1 shuttle vectors carrying an isolated 8-oxodG, Tg, or both of them being adjacent to each other. Our data revealed that the isolated and tandem single-nucleobase lesions exhibited considerably different bypass efficiencies in *E. coli* cells. The tandem lesions are twice as effective as single lesions in blocking DNA replication in AB1157 *E. coli* cells. In addition, the absence of pol IV and pol V, either alone

or in combination, results in an appreciable drop in bypass efficiency of Tg or tandem lesions (Figure 5A). In this context, it is worth noting that Tg does not constitute a replication block in wild-type *E. coli* cells (bypass efficiency ~96%, Figure 5A), which is considerably different from the observation that this lesion inhibits appreciably the DNA replication *in vitro* (41, 42). Our results, however, are in line with the report by Essigmann et al. (59), where no decrease in bypass efficiency was observed for Tg as assessed by using a survival assay with a Tg-bearing single-stranded M13 shuttle vector. Different from the DNA replication *in vitro*, the replication in *E. coli* cells may involve more than one DNA polymerase and the participation of other protein factors (60, 61), which may render a more efficient bypass of the lesion.

The 8-oxodG is mutagenic in all AB1157 strains that we examined. The frequency of G→T transversion mutation is approximately 18%, which is relatively high when compared with the results from recent *in-vivo* replication studies (34,62). However, Basu et al. (20,63) observed that, when the 8-oxodG-bearing shuttle vectors were replicated in COS-7 cells, the lesion induced G→T transversion mutation at frequencies of 23–24% and 6% in 5′-TG*T-3′ and 5′-TG*A-3′ sequence contexts, respectively. Furthermore, molecular modeling results predict that the 8-oxoGua:Ade (‘8-oxoGua’ and ‘Ade’ are 8-oxo-7,8-dihydroguanine and adenine, respectively) base pair stacked relatively poorly with the neighboring 3′ base pair in a 5′-TG*A-3′ sequence when compared with a 5′-TG*T-3′ sequence (63). Therefore, the placement of an 8-oxodG on the 5′ side of thymine could confer an increased mutation frequency for 8-oxodG, which may account for a relatively high frequency of G→T mutation for 8-oxodG in the 5′-CG*T-3′ sequence context used in the present study.

To further confirm the effect of sequence context on the mutation frequency induced by 8-oxodG, we synthesized another 21mer 8-oxodG containing ODN (5′-GTATCCTCCATGGTG*GGCTAT-3′), which has similar sequence context flanking the 8-oxodG site as that used in a recent mutagenesis study (62), and examined the mutation frequency of 8-oxodG in this substrate in AB1157 cells. In this respect, we measured the frequency of the G→T transversion mutation induced by 8-oxodG with LC-MS/MS because the 13mer-G and 13mer-T exhibit very similar mobility on 30% native PAGE (Figure S8A&B). It turned out that the G→T transversion mutation induced by 8-oxodG in this particular sequence (i.e., in TG*G sequence context) dropped to ~5% (Figure S8C), which is consistent with other previous reports showing that 8-oxodG could induce a few percent of G→T transversion while using sequences without a thymine on the 3′ side of the 8-oxodG (34,62). However, the G→T transversion mutation induced by 8-oxodG in CG*T sequence context is ~18% based on the same LC-MS/MS analysis (Figure S8C), which is consistent with the result obtained from native PAGE analysis. Therefore, sequence context also plays an important role on the mutagenic property of 8-oxodG in *E. coli* cells.

Both tandem lesions induced 1.5-fold more G→T mutation at 8-oxodG site compared to single 8-oxodG in wild-type *E. coli* cells as well as in the isogenic AB1157 cells deficient in pol II, pol IV, pol V, or both pol IV and pol V. This result underscored that a neighboring Tg can enhance the mutagenic potential of 8-oxodG.

Together, given the presence of copper ions in normal cells (6) and its cellular accumulation under pathophysiological conditions (64), we believe that the copper-stimulated formation of the 5′-Tg-(8-oxodG)-3′ tandem lesion in DNA exposed with H_2O_2 or γ rays is significant. Although the formation of this type of lesion in cells remains to be assessed, the relatively high frequency of its formation *in vitro* suggests that it might also be induced in cells. The lower *in-vivo* bypass efficiencies and greater mutation frequencies for tandem lesions than their composing individual lesions revealed that, when the two common ROS-induced lesions (i.e., Tg and 8-oxodG) are adjacent to each other, they impose greater cytotoxic and mutagenic

effects by compromising more pronouncedly the efficiency and fidelity of DNA replication in cells.

Supplementary Material

Refer to Web version on PubMed Central for supplementary material.

Acknowledgments

This work was supported by the National Institutes of Health (R01 CA101864). The authors would like to thank Prof. Peter E.M. Gibbs, Prof. John M. Essigmann and Prof. Graham C. Walker for kindly providing the shuttle vector and *E. coli* strains.

References

1. Finkel T, Holbrook NJ. Oxidants, oxidative stress and the biology of ageing. Nature 2000;408:239–247. [PubMed: 11089981]
2. Marnett LJ. Oxyradicals and DNA damage. Carcinogenesis 2000;21:361–370. [PubMed: 10688856]
3. Nikjoo H, O'Neill P, Wilson WE, Goodhead DT. Computational approach for determining the spectrum of DNA damage induced by ionizing radiation. Radiat Res 2001;156:577–583. [PubMed: 11604075]
4. Sutherland BM, Bennett PV, Sutherland JC, Laval J. Clustered DNA damages induced by x rays in human cells. Radiat Res 2002;157:611–616. [PubMed: 12005538]
5. Gulston M, Fulford J, Jenner T, de Lara C, O'Neill P. Clustered DNA damage induced by gamma radiation in human fibroblasts (HF19), hamster (V79-4) cells and plasmid DNA is revealed as Fpg and Nth sensitive sites. Nucleic Acids Res 2002;30:3464–3472. [PubMed: 12140332]
6. Agarwal K, Sharma A, Talukder G. Effects of copper on mammalian cell components. Chem Biol Interact 1989;69:1–16. [PubMed: 2464442]
7. Stoewe R, Prutz WA. Copper-catalyzed DNA damage by ascorbate and hydrogen peroxide: kinetics and yield. Free Radic Biol Med 1987;3:97–105. [PubMed: 2822548]
8. Bach D, Miller IR. Polarographic investigation of binding of Cu^{++} and Cd^{++} by DNA. Biopolymers 1967;5:161–172. [PubMed: 6040714]
9. Bryan SE, Frieden E. Interaction of copper(II) with deoxyribonucleic acid below 30 degrees. Biochemistry 1967;6:2728–2734. [PubMed: 6069709]
10. Prutz WA, Butler J, Land EJ. Interaction of copper(I) with nucleic acids. Int J Radiat Biol 1990;58:215–234. [PubMed: 1974571]
11. Bar-Or D, Winkler JV. Copper is involved in hydrogen-peroxide-induced DNA damage. Free Radic Biol Med 2002;32:197–199. [PubMed: 11796209]
12. Cao H, Wang Y. Quantification of oxidative single-base and intrastrand cross-link lesions in unmethylated and CpG-methylated DNA induced by Fenton-type reagents. Nucleic Acids Res 2007;35:4833–4844. [PubMed: 17626047]
13. Hong H, Cao H, Wang Y. Identification and quantification of a guanine-thymine intrastrand cross-link lesion induced by Cu(II)/H_2O_2/ascorbate. Chem Res Toxicol 2006;19:614–621. [PubMed: 16696563]
14. Lee DH, O'Connor TR, Pfeifer GP. Oxidative DNA damage induced by copper and hydrogen peroxide promotes CG-->TT tandem mutations at methylated CpG dinucleotides in nucleotide excision repair-deficient cells. Nucleic Acids Res 2002;30:3566–3573. [PubMed: 12177298]
15. Drouin R, Rodriguez H, Gao SW, Gebreyes Z, O'Connor TR, Holmquist GP, Akman SA. Cupric ion/ascorbate/hydrogen peroxide-induced DNA damage: DNA-bound copper ion primarily induces base modifications. Free Radic Biol Med 1996;21:261–273. [PubMed: 8855437]
16. Aruoma OI, Halliwell B, Gajewski E, Dizdaroglu M. Copper-ion-dependent damage to the bases in DNA in the presence of hydrogen peroxide. Biochem J 1991;273:601–604. [PubMed: 1899997]
17. Sagripant JL, Kraemer KH. Site-specific oxidative DNA damage at polyguanosines produced by copper plus hydrogen peroxide. J Biol Chem 1989;264:1729–1734. [PubMed: 2912981]

18. Cao H, Jiang Y, Wang Y. Kinetics of deamination and Cu(II)/H_2O_2/Ascorbate-induced formation of 5-methylcytosine glycol at CpG sites in duplex DNA. Nucleic Acids Res 2009;37:6635–6643. [PubMed: 19706732]
19. Gentil A, Le Page F, Cadet J, Sarasin A. Mutation spectra induced by replication of two vicinal oxidative DNA lesions in mammalian cells. Mutat Res 2000;452:51–56. [PubMed: 10894890]
20. Kalam MA, Basu AK. Mutagenesis of 8-oxoguanine adjacent to an abasic site in simian kidney cells: tandem mutations and enhancement of G-->T transversions. Chem Res Toxicol 2005;18:1187–1192. [PubMed: 16097791]
21. Chaudhry MA, Weinfeld M. The action of *Escherichia coli* endonuclease III on multiply damaged sites in DNA. J Mol Biol 1995;249:914–922. [PubMed: 7791217]
22. Venkhataraman R, Donald CD, Roy R, You HJ, Doetsch PW, Kow YW. Enzymatic processing of DNA containing tandem dihydrouracil by endonucleases III and VIII. Nucleic Acids Res 2001;29:407–414. [PubMed: 11139610]
23. Budworth H, Dianov GL. Mode of inhibition of short-patch base excision repair by thymine glycol within clustered DNA lesions. J Biol Chem 2003;278:9378–9381. [PubMed: 12519757]
24. Budworth H, Dianova II, Podust VN, Dianov GL. Repair of clustered DNA lesions. Sequence-specific inhibition of long-patch base excision repair by 8-oxoguanine. J Biol Chem 2002;277:21300–21305. [PubMed: 11923315]
25. Lomax ME, Cunniffe S, O'Neill P. 8-OxoG retards the activity of the ligase III/XRCC1 complex during the repair of a single-strand break, when present within a clustered DNA damage site. DNA Repair 2004;3:289–299. [PubMed: 15177044]
26. Eot-Houllier G, Eon-Marchais S, Gasparutto D, Sage E. Processing of a complex multiply damaged DNA site by human cell extracts and purified repair proteins. Nucleic Acids Res 2005;33:260–271. [PubMed: 15647508]
27. Wang Y. Bulky DNA lesions induced by reactive oxygen species. Chem Res Toxicol 2008;21:276–281. [PubMed: 18189366]
28. Box HC, Budzinski EE, Dawidzik JB, Gobey JS, Freund HG. Free radical-induced tandem base damage in DNA oligomers. Free Radic Biol Med 1997;23:1021–1030. [PubMed: 9358245]
29. Box HC, Budzinski EE, Dawidzik JB, Wallace JC, Iijima H. Tandem lesions and other products in X-irradiated DNA oligomers. Radiat Res 1998;149:433–439. [PubMed: 9588353]
30. Zhang Q, Wang Y. Generation of 5-(2′-deoxycytidyl)methyl radical and the formation of intrastrand cross-link lesions in oligodeoxyribonucleotides. Nucleic Acids Res 2005;33:1593–1603. [PubMed: 15767284]
31. Bellon S, Ravanat JL, Gasparutto D, Cadet J. Cross-linked thymine-purine base tandem lesions: synthesis, characterization, and measurement in gamma-irradiated isolated DNA. Chem Res Toxicol 2002;15:598–606. [PubMed: 11952347]
32. Bourdat AG, Douki T, Frelon S, Gasparutto D, Cadet J. Tandem base lesions are generated by hydroxyl radical within isolated DNA in aerated aqueous solution. J Am Chem Soc 2000;122:4549–4556.
33. Gu C, Wang Y. LC-MS/MS identification and yeast polymerase η bypass of a novel γ-irradiation-induced intrastrand cross-link lesion G[8–5]C. Biochemistry 2004;43:6745–6750. [PubMed: 15157108]
34. Hong H, Cao H, Wang Y. Formation and genotoxicity of a guanine-cytosine intrastrand cross-link lesion *in vivo*. Nucleic Acids Res 2007;35:7118–7127. [PubMed: 17942427]
35. Hong IS, Carter KN, Sato K, Greenberg MM. Characterization and mechanism of formation of tandem lesions in DNA by a nucleobase peroxyl radical. J Am Chem Soc 2007;129:4089–4098. [PubMed: 17335214]
36. Jiang Y, Hong H, Cao H, Wang Y. *In vivo* formation and *in vitro* replication of a guanine-thymine intrastrand cross-link lesion. Biochemistry 2007;46:12757–12763. [PubMed: 17929946]
37. Budzinski EE, Dawidzik JD, Wallace JC, Freund HG, Box HC. The radiation chemistry of d (CpGpTpA) in the presence of oxygen. Radiat Res 1995;142:107–109. [PubMed: 7899553]
38. Box HC. Double lesions are produced in DNA oligomer by ionizing radiation and by metal-catalyzed H_2O_2 reactions. Radiat Res 2001;155:634–636. [PubMed: 11260666]

39. Hayes RC, Petrullo LA, Huang HM, Wallace SS, LeClerc JE. Oxidative damage in DNA. Lack of mutagenicity by thymine glycol lesions. J Mol Biol 1988;201:239–246. [PubMed: 3418701]
40. Collins AR. Oxidative DNA damage, antioxidants, and cancer. Bioessays 1999;21:238–246. [PubMed: 10333733]
41. McNulty JM, Jerkovic B, Bolton PH, Basu AK. Replication inhibition and miscoding properties of DNA templates containing a site-specific *cis*-thymine glycol or urea residue. Chem Res Toxicol 1998;11:666–673. [PubMed: 9625735]
42. Ide H, Kow YW, Wallace SS. Thymine glycols and urea residues in M13 DNA constitute replicative blocks *in vitro*. Nucleic Acids Res 1985;13:8035–8052. [PubMed: 3906566]
43. Shibutani S, Takeshita M, Grollman AP. Insertion of specific bases during DNA synthesis past the oxidation-damaged base 8-oxodG. Nature 1991;349:431–434. [PubMed: 1992344]
44. Cheng KC, Cahill DS, Kasai H, Nishimura S, Loeb LA. 8-Hydroxyguanine, an abundant form of oxidative DNA damage, causes G-->T and A-->C substitutions. J Biol Chem 1992;267:166–172. [PubMed: 1730583]
45. Bienvenu C, Cadet J. Synthesis and kinetic study of the deamination of the *cis* diastereomers of 5,6-dihydroxy-5,6-dihydro-5-methyl-2′-deoxycytidine. J Org Chem 1996;61:2632–2637. [PubMed: 11667092]
46. Zuo S, Boorstein RJ, Teebor GW. Oxidative damage to 5-methylcytosine in DNA. Nucleic Acids Res 1995;23:3239–3243. [PubMed: 7667100]
47. Jiang Y, Wang Y, Wang Y. In vitro replication and repair studies of tandem lesions containing neighboring thymidine glycol and 8-oxo-7,8-dihydro-2′-deoxyguanosine. Chem Res Toxicol 2009;22:574–583. [PubMed: 19193190]
48. Gibbs PE, Kilbey BJ, Banerjee SK, Lawrence CW. The frequency and accuracy of replication past a thymine-thymine cyclobutane dimer are very different in *Saccharomyces cerevisiae* and *Escherichia coli*. J Bacteriol 1993;175:2607–2612. [PubMed: 8478326]
49. Jarosz DF, Beuning PJ, Cohen SE, Walker GC. Y-family DNA polymerases in *Escherichia coli*. Trends Microbiol 2007;15:70–77. [PubMed: 17207624]
50. Wang Y, Wang Y. Synthesis and thermodynamic studies of oligodeoxyribonucleotides containing tandem lesions of thymidine glycol and 8-oxo-2′-deoxyguanosine. Chem Res Toxicol 2006;19:837–843. [PubMed: 16780363]
51. Delaney JC, Essigmann JM. Assays for determining lesion bypass efficiency and mutagenicity of site-specific DNA lesions *in vivo*. Methods Enzymol 2006;408:1–15. [PubMed: 16793359]
52. Delaney JC, Essigmann JM. Mutagenesis, genotoxicity, and repair of 1-methyladenine, 3-alkylcytosines, 1-methylguanine, and 3-methylthymine in alkB *Escherichia coli*. Proc Natl Acad Sci U S A 2004;101:14051–14056. [PubMed: 15381779]
53. Delaney JC, Essigmann JM. Context-dependent mutagenesis by DNA lesions. Chem Biol 1999;6:743–753. [PubMed: 10508678]
54. Yuan B, Cao H, Jiang Y, Hong H, Wang Y. Efficient and accurate bypass of N^2-(1-carboxyethyl)-2′-deoxyguanosine by DinB DNA polymerase *in vitro* and *in vivo*. Proc Natl Acad Sci U S A 2008;105:8679–8684. [PubMed: 18562283]
55. Yuan B, Wang Y. Mutagenic and cytotoxic properties of 6-thioguanine, S^6-methylthioguanine, and guanine-S^6-sulfonic acid. J Biol Chem 2008;283:23665–23670. [PubMed: 18591241]
56. Wang Y. HPLC isolation and mass spectrometric characterization of two isomers of thymine glycols in oligodeoxynucleotides. Chem Res Toxicol 2002;15:671–676. [PubMed: 12018988]
57. Huang H, Imoto S, Greenberg MM. The mutagenicity of thymidine glycol in *Escherichia coli* is increased when it is part of a tandem lesion. Biochemistry 2009;48:7833–7841. [PubMed: 19618962]
58. Davis AV, O'Halloran TV. A place for thioether chemistry in cellular copper ion recognition and trafficking. Nat Chem Biol 2008;4:148–151. [PubMed: 18277969]
59. Basu AK, Loechler EL, Leadon SA, Essigmann JM. Genetic effects of thymine glycol: site-specific mutagenesis and molecular modeling studies. Proc Natl Acad Sci U S A 1989;86:7677–7681. [PubMed: 2682618]
60. Sutton MD, Walker GC. Managing DNA polymerases: coordinating DNA replication, DNA repair, and DNA recombination. Proc Natl Acad Sci USA 2001;98:8342–8349. [PubMed: 11459973]

61. Maga G, Villani G, Crespan E, Wimmer U, Ferrari E, Bertocci B, Hubscher U. 8-oxo-guanine bypass by human DNA polymerases in the presence of auxiliary proteins. Nature 2007;447:606–608. [PubMed: 17507928]

62. Neeley WL, Delaney S, Alekseyev YO, Jarosz DF, Delaney JC, Walker GC, Essigmann JM. DNA polymerase V allows bypass of toxic guanine oxidation products *in vivo*. J Biol Chem 2007;282:12741–12748. [PubMed: 17322566]

63. Kalam MA, Haraguchi K, Chandani S, Loechler EL, Moriya M, Greenberg MM, Basu AK. Genetic effects of oxidative DNA damages: Comparative mutagenesis of the imidazole ring-opened formamidopyrimidines (Fapy lesions) and 8-oxo-purines in simian kidney cells. Nucleic Acids Res 2006;34:2305–2315. [PubMed: 16679449]

64. Ala A, Walker AP, Ashkan K, Dooley JS, Schilsky ML. Wilson's disease. Lancet 2007;369:397–408. [PubMed: 17276780]

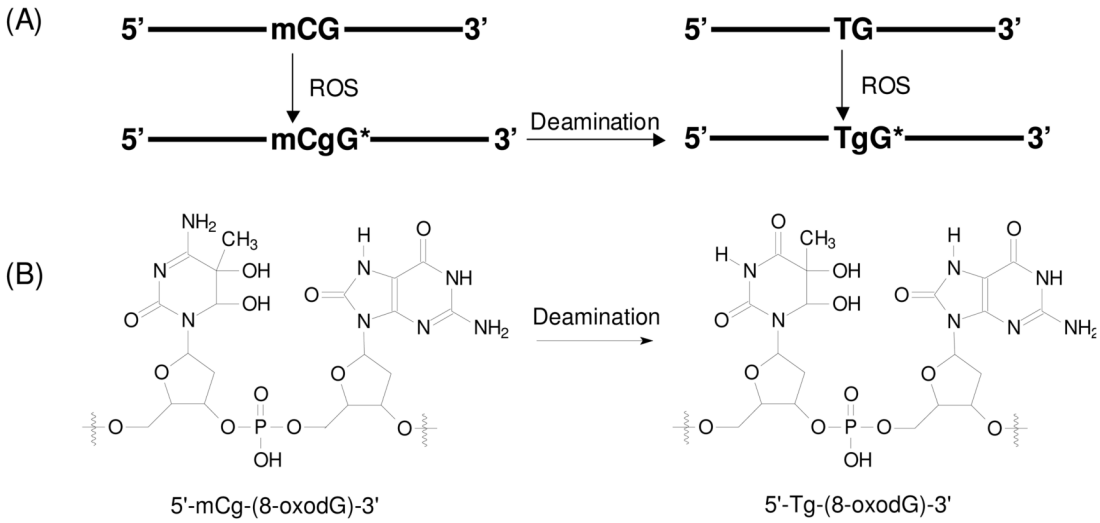

Figure 1. The formation of the 5′-Tg-(8-oxodG)-3′ tandem lesion

G*, mC, and mCg represent 8-oxoGua, 5-methylcytosine and 5-methylcytosine glycol, respectively.

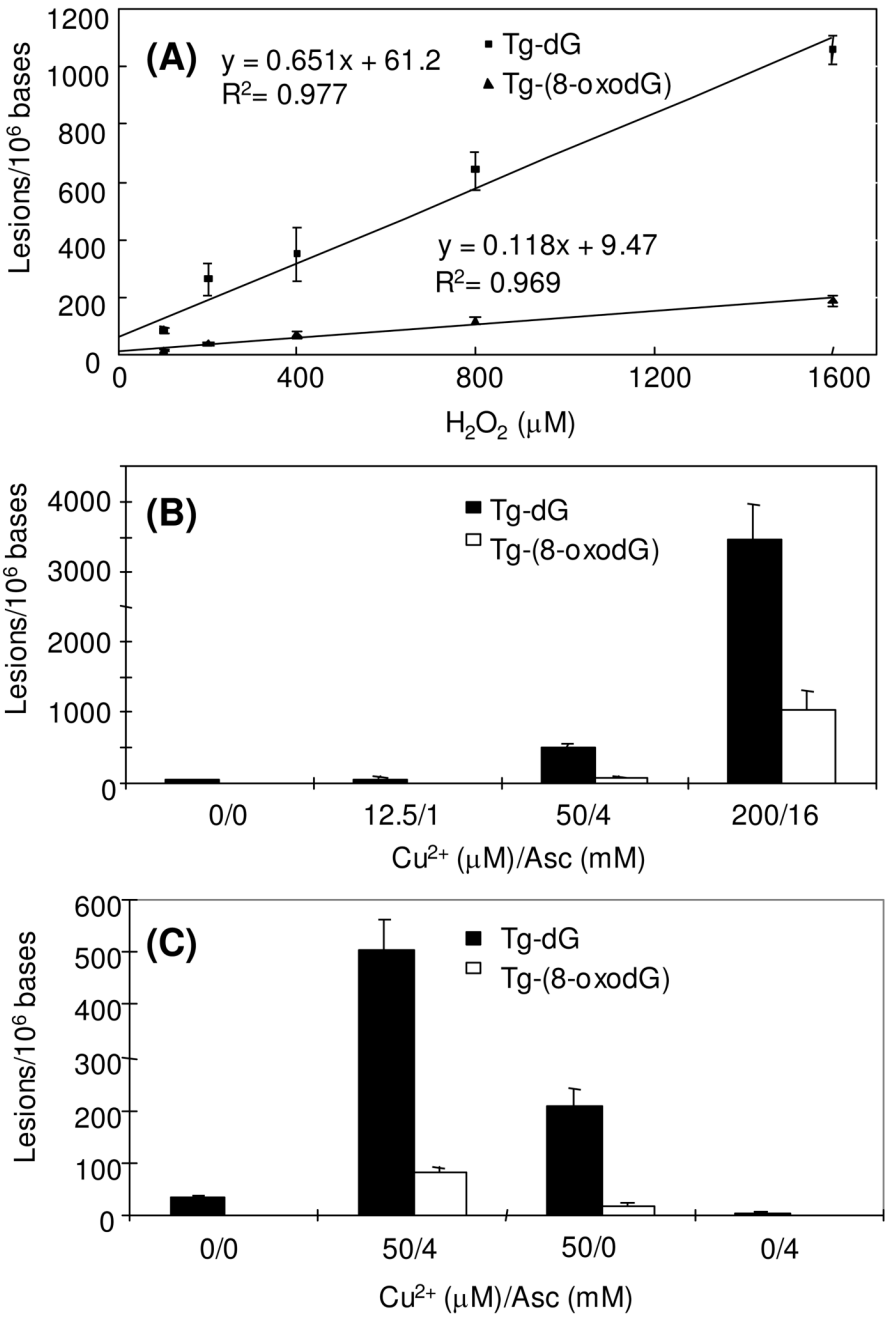

Figure 2. The quantitative formation of the 5′-Tg-dG-3′ and 5′-Tg-(8-oxodG)-3′ lesions in calf thymus DNA exposed with Cu(II) and ascorbate along with H_2O_2 or γ rays

(A) Dose-dependent induction of the 5′-Tg-dG-3′ and 5′-Tg-(8-oxodG)-3′ lesions in calf thymus DNA by Cu(II)/H_2O_2/ascorbate. (B) The induction of 5′-Tg-dG-3′ and 5′-Tg-(8-oxodG)-3′ lesions in calf-thymus DNA upon exposure to 50 Gy of γ rays in combination with Cu(II) and ascorbate at the indicated concentrations. (C) The induction of 5′-Tg-dG-3′ and 5′-Tg-(8-oxodG)-3′ lesions in calf thymus DNA upon treatment with 50 Gy of γ rays, alone or in combination with 50 μM Cu(II), 4 mM ascorbic acid, or both. The data represent the means ± S.D. of results from three independent treatments and LC-MS/MS quantification experiments.

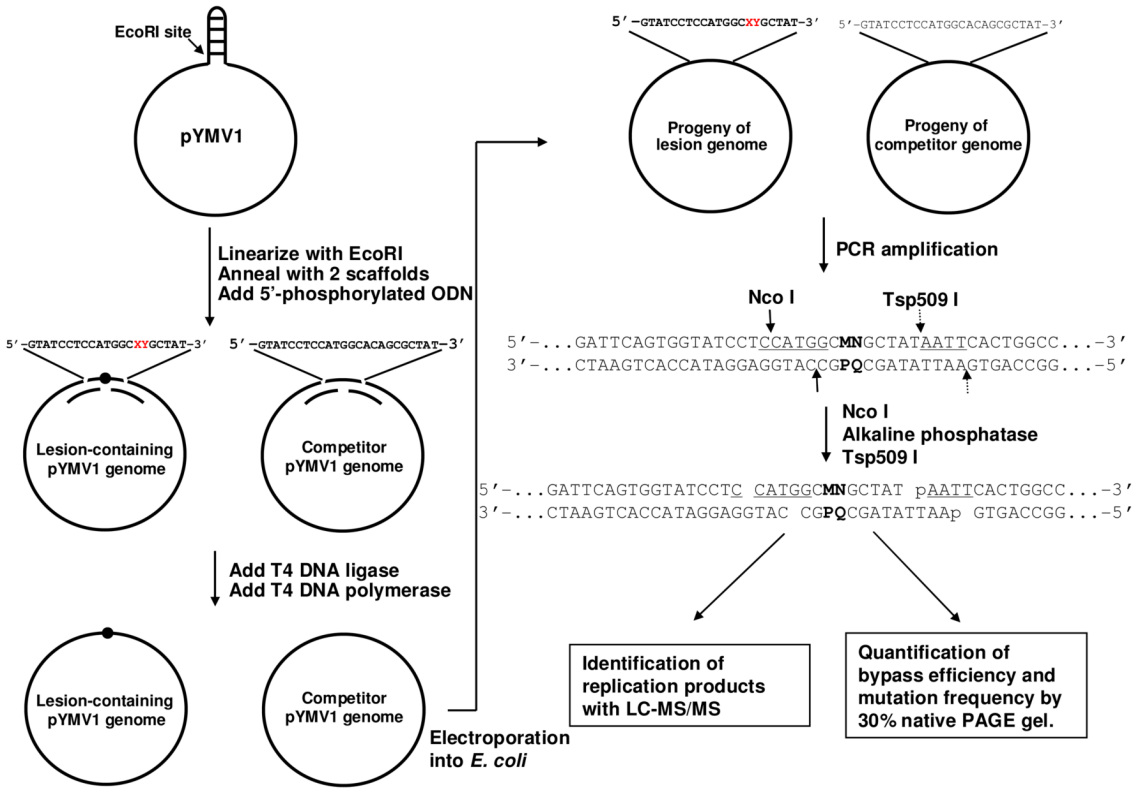

Figure 3. The method for the determination of the cytotoxicity and mutagenicity of DNA lesions in *E. coli* cells

'XY' in the 21mer ODN represents 5′-(8-oxodG)-dT-3′ (**G*****T**), 5′-Tg-dG-3′ (**TgG**), 5′-(8-oxodG)-Tg-3′ (**G*****Tg**) and 5′-Tg-(8-oxodG)-3′ (**TgG***). 'MN' in the progeny of the lesion genome represents the nucleotides inserted at the above dinucleotide site. NcoI and Tsp509I restriction endonuclease recognition sites are underlined and the cleavage sites induced by the two enzymes are designated by solid and broken arrows, respectively. Only partial sequence of PCR products for the lesion genome is shown, and the PCR products of the competitor genome are not shown.

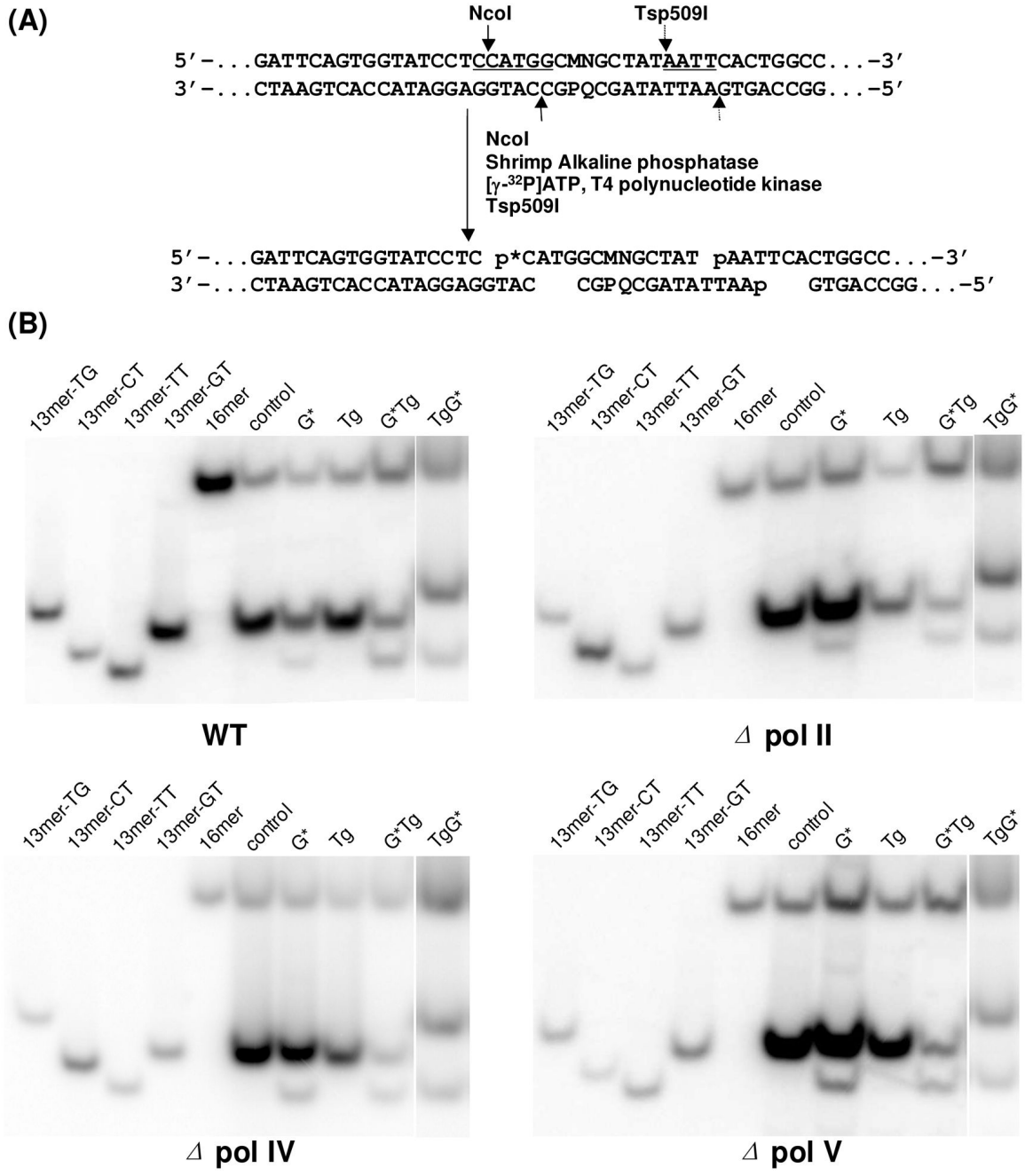

Figure 4. Measurement of the *in vivo* bypass efficiencies and mutation frequencies by the CRAB and REAP assay

(A) Sample processing ('p*' represents the ^{32}P-labeled phosphate group); (B) gel image showing the 16mer and 13mer ODNs released from the PCR products of the progeny resulting from the replication of the competitor genome and the control or lesion-carrying genome in wild-type and the isogenic AB1157 cells deficient in pol II, pol IV or pol V. The restriction fragment arising from the competitor genome, i.e., d(CATGGCACAGCGCTAT), is designated with '16mer'; '13mer-GT', '13mer-TT', '13mer-CT' and '13mer-TG' represent standard ODNs d(CATGGC**MN**GCTAT), where 'MN' are 'GT', 'TT', 'CT' and 'TG', respectively. 'G*' represents 8-oxodG. The right lane in each gel panel was separated from

other lanes because we carried out the CRAB and REAP assays for the 5′-Tg-(8-oxodG)-3′ tandem lesion at a different time. Figure S10 showed the image of the gel for the separation of standard ODNs along with the replication products of the 5′-Tg-(8-oxodG)-3′ tandem lesion in wild-type and the isogenic AB1157 cells deficient in SOS-induced polymerase(s).

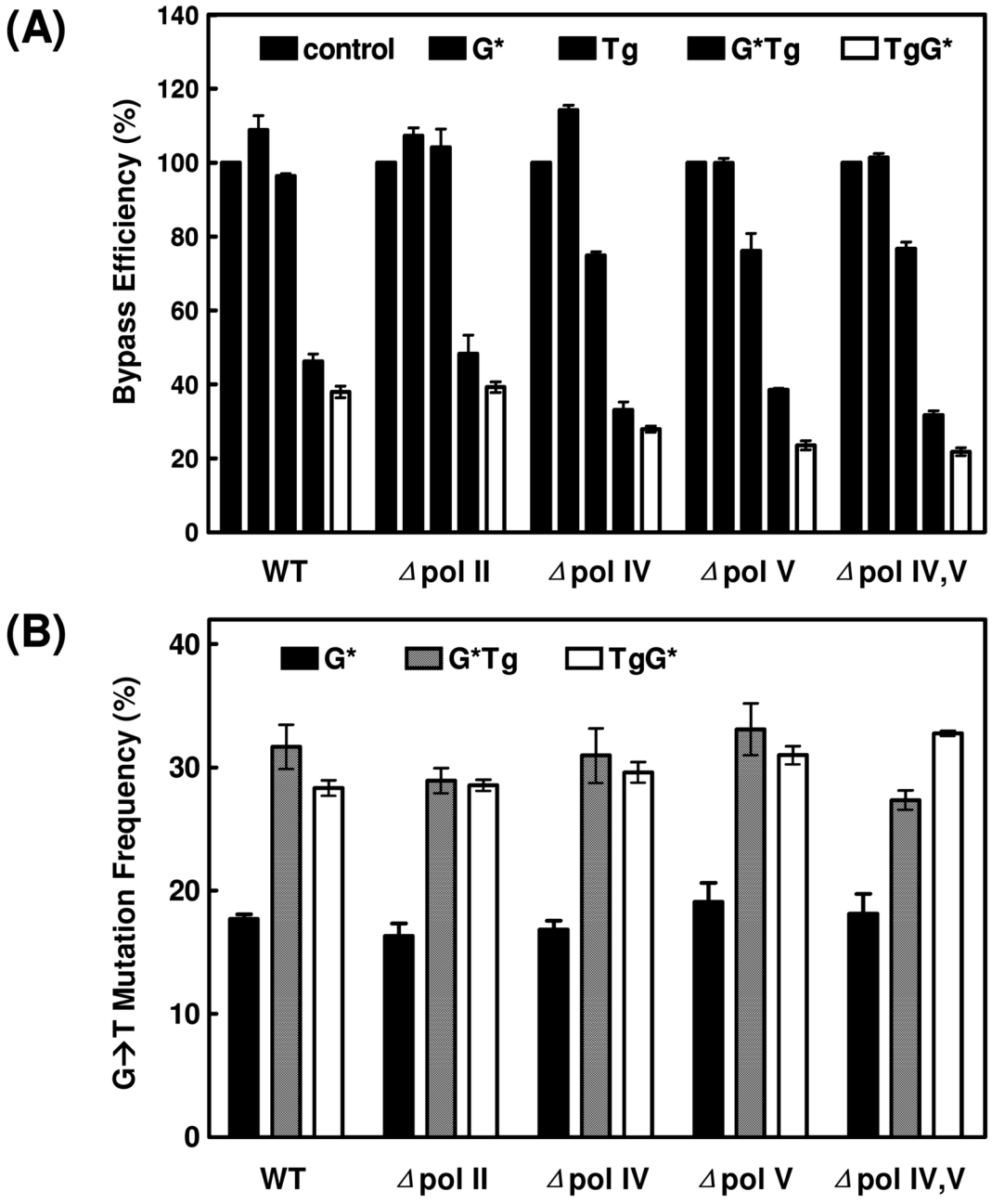

Figure 5. Bypass efficiencies (A) and mutation frequencies (B) of 8-oxodG and Tg, present alone or in tandem, in wild-type and polymerase-deficient AB1157 *E. coli* cells

Shown are the results for the substrates carrying unmodified GT, an isolated 8-oxodG (G*), an isolated Tg (Tg), 5′-(8-oxodG)-Tg-3′ (G*Tg) and 5′-Tg-(8-oxodG)-3′ (TgG*), respectively. 'Ctrl' designates the control substrate. The data represent the means and standard deviations of results from three independent experiments. The *p*-values for comparing the difference in bypass efficiencies of various lesions in wild-type versus polymerase-deficient AB1157 strains are shown in Table S2.

Table 1

Concentrations of Fenton-type reagents employed for the treatment of calf thymus DNA[a]

	Control	A	B	C	D	E
$CuCl_2$ (μM)	0	12.5	25.0	50.0	100	200
H_2O_2 (μM)	0	100	200	400	800	1600
Ascorbate (mM)	0	1.0	2.0	4.0	8.0	16

[a]All reactions were carried out in a 500 μL solution containing 150 μg of calf thymus DNA.